applied sciences

MDPI

Article

An Improved AoT-DCGAN and T-CNN Hybrid Deep Learning Model for Intelligent Diagnosis of PTCs Quality under Small Sample Space

Zihan Ma [1], Yuxiang Chen [1,*], Yu Fan [2], Xiaohai He [3], Wei Luo [2] and Jun Shu [3]

[1] Department of Mechanical Engineering, Southwest Petroleum University, Chengdu 610500, China; ziihanm@163.com
[2] Engineering Technology Research Institute of Petrochina Southwest Oil and Gas Field Company, Chengdu 610000, China
[3] College of Electronics and Information Engineering, Sichuan University, Chengdu 610065, China
* Correspondence: cyx@swpu.edu.cn

Abstract: The intelligent diagnosis of premium threaded connections (PTCs) is vital for ensuring the robust and leak-proof performance of tubing under high-temperature, high-pressure, acidic gas conditions. However, achieving accurate diagnostic results necessitates a substantial number of PTCs curves under diverse make-up conditions, presenting considerable challenges in practical industrial detection. In this study, we introduce an end-to-end classification model, which combines an asynchronously optimized two-dimensional deep convolutional generative adversarial network (AoT-DCGAN) and a two-dimensional convolutional neural network (T-CNN), designed to enhance the classification performance under small sample size. Our proposed method first leverages AoT-DCGAN to identify the distribution patterns of the original samples and generate synthetic counterparts. Concurrently, we implement a novel weight optimization strategy, termed asynchronous optimization (AO), to alleviate the issue of gradient vanishing during the generator's optimization phase. Following this, a novel T-CNN model is devised and trained on the enlarged dataset to automate the classification of PTCs curves. The performance evaluation of our method, based on recall, specificity, F1-score, precision values, and confusion matrices at varying data augmentation ratios, demonstrates that the model's classification capabilities are enhanced as the dataset size escalates, peaking at a dataset size of 1200. Moreover, given the same training set, the T-CNN model outperforms traditional machine learning and deep learning models, achieving classification accuracies of up to 95.9%, 95.5%, and 96.7% for the AC, ATI, and NDT curves, respectively. Lastly, it was confirmed that applying asynchronous optimization in the DCGAN training process results in a more consistent decline in the loss function.

Keywords: premium threaded connections; convolutional neural network; generative adversarial network; small samples; asynchronous optimization

check for updates

Citation: Ma, Z.; Chen, Y.; Fan, Y.; He, X.; Luo, W.; Shu, J. An Improved AoT-DCGAN and T-CNN Hybrid Deep Learning Model for Intelligent Diagnosis of PTCs Quality under Small Sample Space. *Appl. Sci.* **2023**, *13*, 8699. https://doi.org/10.3390/app13158699

Academic Editor: Ki-Yong Oh

Received: 3 July 2023
Revised: 26 July 2023
Accepted: 26 July 2023
Published: 27 July 2023

Copyright: © 2023 by the authors. Licensee MDPI, Basel, Switzerland. This article is an open access article distributed under the terms and conditions of the Creative Commons Attribution (CC BY) license (https://creativecommons.org/licenses/by/4.0/).

1. Introduction

Premium threaded connections (PTCs) play a vital role in preventing the leakage of high-temperature, high-pressure, and hydrogen sulfide gases from tubing into the atmosphere [1–3]. The interference fit between the threads creates a gas-tight seal, but even minor damage during transportation or improper connections can compromise this seal, leading to environmental damage and economic losses. Therefore, diagnosing the connection quality of PTCs is crucial to prevent leaks. The current primary method involves the manual inspection of torque curves generated during PTC connections to identify damage or correct connections [4–7]. However, manual inspection relies heavily on the professional background and work experience of field engineers, leading to a lack of objectivity and quantifiability in the evaluation [8]. Therefore, achieving intelligent diagnosis of PTCs quality necessitates automatic classification and recognition of PTCs curves under different connection conditions.

In recent years, artificial intelligence (AI) applications and research across various industries have significantly improved the diagnosis of PTCs quality. Ma et al. [9] introduced a machine learning method based on logistic regression for PTCs curve classification, achieving an initial intelligent recognition capability by categorizing curves into qualified and unqualified classes. Although this method reveals statistical and spatial feature distribution characteristics under varying conditions, it relies heavily on manual feature extraction. This dependency becomes a challenge, as improper feature extraction can considerably affect the model's classification outcomes. In contrast, deep learning through multi-layer neural networks automatically learns high-level feature representations from raw data, eliminating the laborious process of manual feature engineering [10]. Thus, the application of deep learning for the automatic classification of PTCs curves emerges as a promising solution to the current issues.

Recently, considerable research on and applications of deep learning has been conducted for tasks such as target classification and recognition in areas including medicine, biology, and mechanical engineering. The use of convolutional neural networks (CNNs) has gained particular attention due to their unique convolutional operations and global weight-sharing mechanism, achieving state-of-the-art classification performance [11–17]. Peng et al. [18] proposed a deep learning-based intelligent method for monitoring and diagnosing the working conditions of sucker-rod pumping wells. This approach used deep convolutional neural network algorithms to analyze the relationship between electrical data and dynamometer cards under different working conditions, artificially synthesizing dynamometer cards. The researcher also employed convolutional neural networks to automatically diagnose the artificially synthesized dynamometer cards, achieving prediction accuracy exceeding 95%. Zhang et al. [19] combined convolutional neural networks and transfer learning methods. The pretrained network model was trained on a dynamometer card dataset with ten different working conditions, leading to the intelligent diagnosis of dynamometer card conditions. The recognition accuracy reached 92.6%, outperforming general fully connected neural networks and shallow convolutional neural networks. Tang et al. [20] applied a convolutional neural network model to classify and recognize the original vibration data, frequency spectrum data, and time-frequency data of gearboxes. The results demonstrated that the neural network model could automatically learn key features from frequency domain data and intelligently diagnose gearbox faults.

However, the aforementioned research on classification and recognition tasks based on convolutional neural networks typically assumes the availability of ample training data. In this study, the focus is on classifying PTCs curves under different connection conditions, making this assumption challenging. Only a small fraction of PTCs may experience thread damage or improper connections, making the acquisition of a substantial number of corresponding PTCs curves exceedingly difficult. Hence, it is crucial to develop an intelligent diagnostic method that can effectively classify PTC curves under a small sample size.

A viable solution to handle the issue of an insufficient training dataset is data augmentation. Generally, data augmentations can artificially inflate the training dataset by either data warping or oversampling [21,22]. Data warping refers to introducing real-world distortions, such as elastic deformation, random cropping, rotation, and scaling, into the training data. In contrast, oversampling augmentations generate entirely new samples to supplement the original training dataset. The generative adversarial network (GAN), as one of the most innovative oversampling augmentations, has gained considerable attention since its introduction in 2014 [23]. Unlike other data augmentation techniques, GAN learns the distribution patterns of samples in the training dataset and generates synthetic specimens with the original features. Numerous studies have shown that GAN has been receiving increasing attention in the field of small-sample fault diagnosis, achieving promising results [24–29]. Zhang et al. [26] presented a multi-module gradient penalized GAN to address small sample problems in the intelligent fault diagnosis schemes of machines. The GAN's generator can create mechanical signals under different conditions and further expand the training dataset, improving the classification performance. Wang et al. [30] proposed an enhanced generative adversarial network (E-GAN), which employs a deep convolutional generative adversarial network (DCGAN) to balance the data and a modified CNN diagnosis model for fault classification. Li et al. [31] addressed the issue of imbalanced distribution of fault samples in rotating machinery by proposing an auxiliary classifier Wasserstein generative adversarial network (ACWGAN), which is capable of generating high-quality samples for minority classes.

Inspired by the success of deep learning in various domains of classification tasks and its potential in data augmentation, this paper proposes an improved AoT-DCGAN and T-CNN hybrid deep learning model for the intelligent recognition of PTCs curves under small samples. The proposed method consists of two stages: data generation and curve classification. The first stage involves building an AoT-DCGAN model to learn the feature distribution from original PTCs curves and generate synthetic samples to inflate the training dataset. The second stage proposes a T-CNN model for classifying PTCs curves, trained using an augmented dataset. The results are compared with datasets at different augmentation ratios and traditional machine learning models to validate the superiority of the proposed method in terms of classification performance.

The main contributions of this paper are as follows:

(1) We design a hybrid deep learning model for the automatic classification of PTCs curves. The model achieves good classification results under small samples, enabling the fast and quantitative evaluation of the connection quality of PTCs.
(2) We propose an AoT-DCGAN model capable of generating samples that closely resemble real PTCs curves, exhibiting high authenticity and accuracy. Furthermore, the model training process is more stable, effectively addressing the issue of gradient vanishing.
(3) We introduce a T-CNN model for classifying PTCs curves which achieves superior classification performance compared to traditional machine learning and deep learning models.

The organization of this paper is as follows. In Section 2, the basic concepts of the dataset used in this study are described. An overview of the proposed AoT-DCGAN and T-CNN hybrid deep learning models is provided, along with a detailed description of a novel weight optimization strategy. Section 3 demonstrates the results of the proposed model by comparing the classification performance at different augmentation ratios and using traditional machine learning models. Section 4 concludes the paper and discusses future directions for research.

2. Materials and Methods

This section delivers a detailed account of the origins and character of the dataset utilized in this study. Further, we outline the structure and fundamental principles of the proposed hybrid deep learning model.

2.1. PTCs Curve

Different from API tubing connections, the unique metal-to-metal seal design and torque shoulder of PTCs notably improve the gas sealing performance of the tubing, effectively eliminating the possibility of gas leakage under complex loads [32,33]. The make-up torque curve of PTCs, also referred to as the PTCs curve, serves as a crucial indicator of the proper connection of PTCs. It is generated by logging and analyzing the torque and turns data during the premium threaded connections tubing make-up process. As the threaded tubing is progressively tightened, the applied force and torque gradually increase until a particular resistance is met. Figure 1 visualizes the structural features of PTCs and the torque curve demonstrated at each stage of the make-up process.

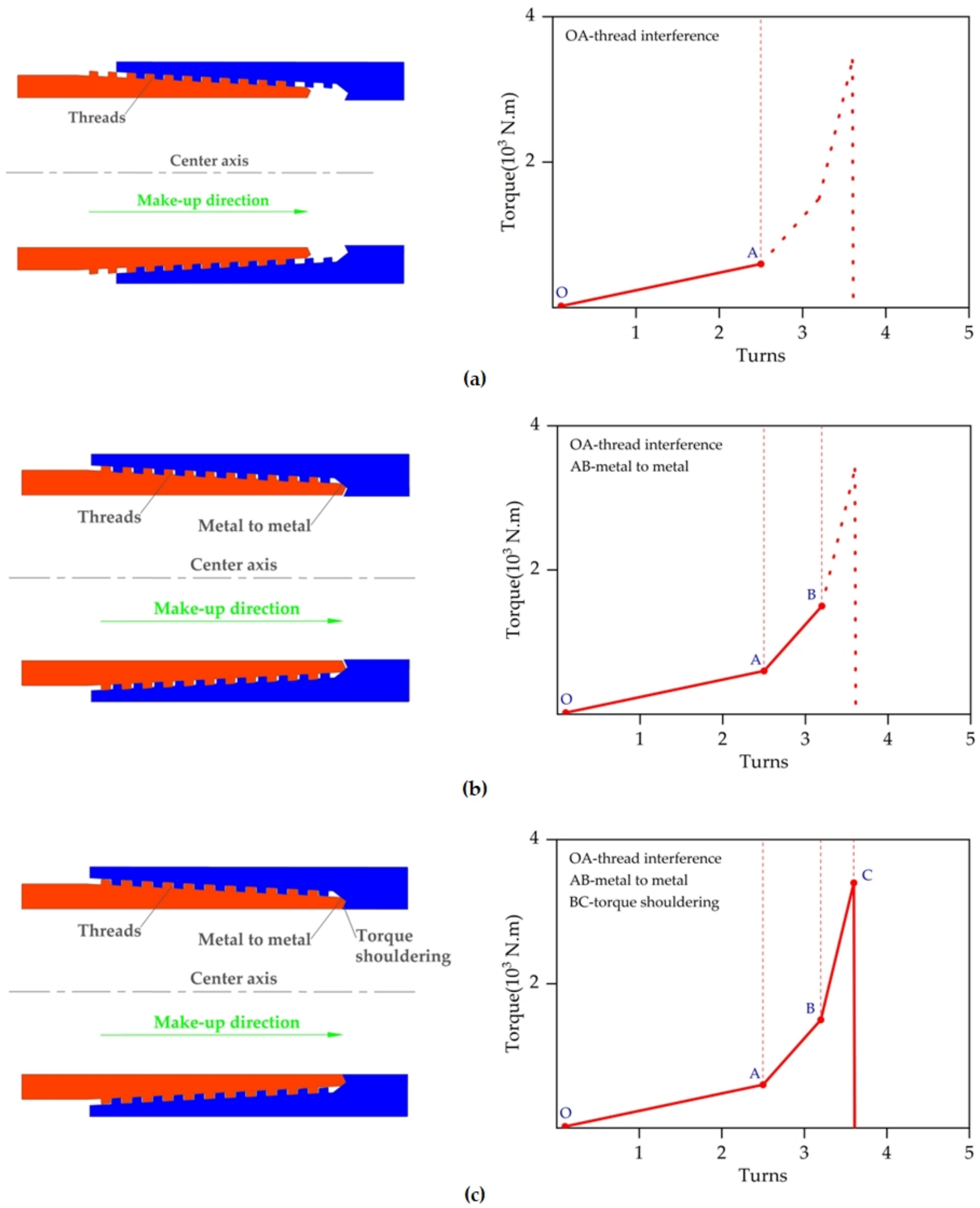

Figure 1. PTCs and corresponding torque curves for different make-up stages: (**a**) thread interference; (**b**) metal-to-metal section; (**c**) torque shouldering section.

As depicted in Figure 1, in the initial make-up stage, the primary resistance originates from the friction among the threads, leading to a PTCs curve shown by the solid red line in Figure 1a, called the "thread interference section". Once all thread segments make contact, the metal-to-metal sealing phase commences, causing a notable rise in the torque curve, as demonstrated by the red solid line in Figure 1b, termed the "metal-to-metal section." When the metal-to-metal section achieves a certain level, the torque shoulder activates to prevent excessive metal contact. Consequently, the torque curve quickly rises until the complete make-up process concludes, as depicted by the solid red line in Figure 1c, dubbed the "torque shouldering section." Hence, a typical make-up torque curve exhibits three phases: gradual increase, significant increase, and rapid increase, representing the thread interference, metal-to-metal sealing, and torque shouldering sections, respectively [8]. However, during real make-up processes, abnormalities in the PTCs curve may appear due to misalignment or thread damage, as demonstrated in Figure 2b,c. This paper aims to intelligently evaluate the connection quality of PTCs by automatically recognizing these three types of PTCs curves.

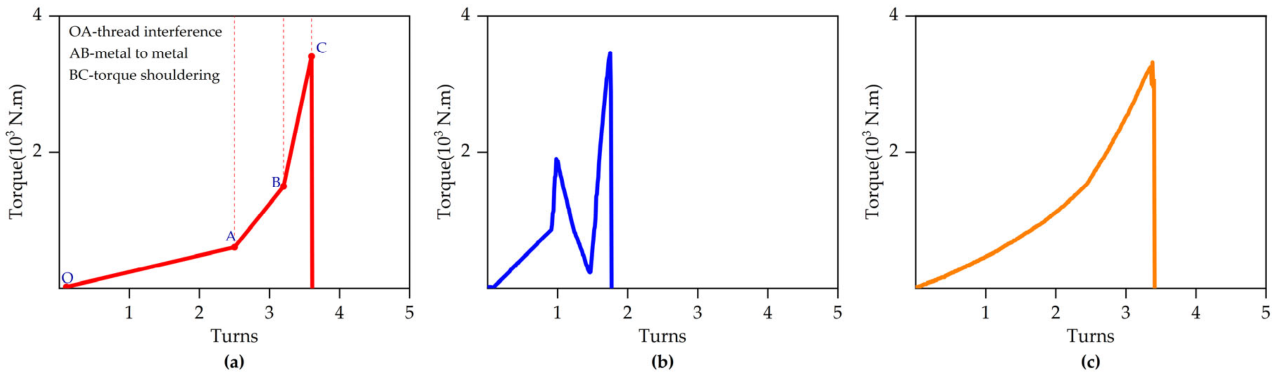

Figure 2. Typical PTCs curves under different make-up conditions: (**a**) standard PTCs curve; (**b**) misalignment PTCs curve; (**c**) thread damage PTCs curve.

2.2. Proposed Method

This paper introduces an improved AoT-DCGAN and T-CNN hybrid deep learning model suitable for classification tasks under small sample sizes. The model merges the ratios of the data generation network (DCGAN) and the classification network (CNN). Firstly, the AoT-DCGAN is employed to learn the underlying distribution patterns within the PTCs curves to generate extra samples. This is achieved by establishing mapping from the noise vectors to the real data distribution. By utilizing this mapping, more artificial curve samples can be generated from random noise, effectively augmenting the dataset. Subsequently, the T-CNN extracts features from these augmented samples and performs classification. Figure 3 illustrates the overview of this hybrid model, providing a visual representation of its architecture. In this workflow diagram, the left diagram represents the data generation process, while the right diagram represents the classification process.

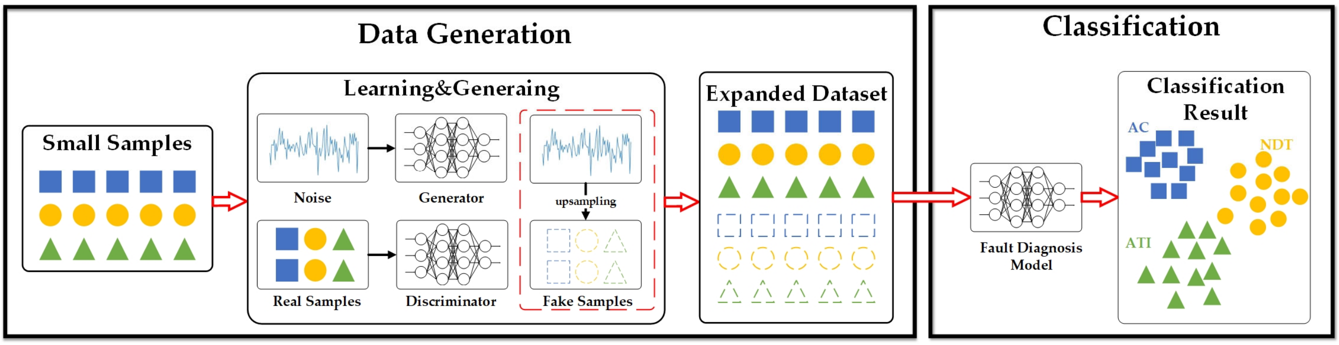

Figure 3. Workflow of proposed hybrid deep learning model.

2.2.1. The Structure of the AoT-DCGAN Model

In this study, we introduce an AoT-DCGAN model, composed of a two-dimensional DCGAN model and an asynchronous optimization (AO) strategy. As illustrated in Figure 4, the AoT-DCGAN's generator includes six two-dimensional deconvolutional layers, while the discriminator is composed of five two-dimensional convolutional layers. The generator inputs a 100-dimensional random noise vector z and up-scales it through a series of deconvolutional layers to generate data of the same size as the real samples [34]. The discriminator's process is similar to that of a convolutional neural network performing a classification task. It down-samples and extracts features from both real and synthetic samples, and the output layer produces a scalar of dimension 1, indicating the input sample's probability of being real. A higher output value close to 1 suggests a more realistic sample.

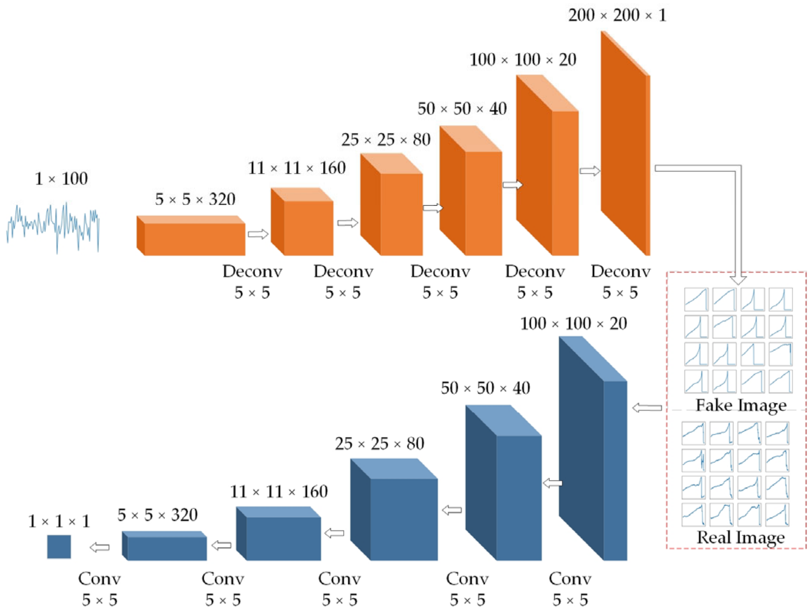

Figure 4. The detailed structure of AoT-DCGAN.

For the generator and discriminator to reach a Nash equilibrium state, in which the generator produces realistic samples indistinguishable by the discriminator from real specimens, and in which the discriminator performs well in distinguishing the generated samples, the generator and discriminator's weights require separate optimization using different algorithms. The discriminator's objective is to minimize the loss function calculated using the binary cross-entropy function for both real and synthetic samples, as shown in Equation (1). Conversely, the generator aims to minimize the negative logarithm of the probability of fake samples classified as real by the discriminator, as shown in Equation (2). During the training process, these results are used to update the weights of the corresponding neurons in the network through backpropagation.

$$L_{discriminator} = -\log D(real\_sample) - \log(1 - D(G(fake\_sample))) \tag{1}$$

$$L_{generator} = -\log(D\Big(G\Big(fake_{sample}\Big)\Big)\Big) \tag{2}$$

where D and G represents the discriminator and generator; x is the real sample from the training dataset, and z is a random noise input. $G\ (z)$ maps z to the data space to fit the statistical distribution of the real sample, while $D\ (x)$ obtains the probability of the input data.

However, during the model's initial training stages, the discriminator may excessively dominate, making it difficult for the generator to acquire effective gradient signals to update its neuron weights. Consequently, the generator may get stuck in a local optimum, generating a limited set of samples that the discriminator cannot recognize, without covering the entire data distribution. To mitigate these issues, the proposed asynchronous optimization (AO) updates the generator's weights at each iteration of the backpropagation process, while the discriminator's weights are updated every four iterations. Furthermore, the weights used to update the discriminator are obtained by averaging the weight changes over four iterations in the cycle. The specific optimization scheme for the discriminator's weights is shown in Figure 5, and the weight update formula for the discriminator is as follows:

$$W_D = \frac{1}{n}\sum_{i}^{n}\frac{\partial_{loss(i)}}{\partial_{l(i)}} \tag{3}$$

where, the $loss(i)$ represents the loss function of the discriminator in the i-th iteration, and $l(i)$ represents the weight parameters in the i-th iteration. The variable n represents the number of iterations for weight updates, while we set n as 4 in this study.

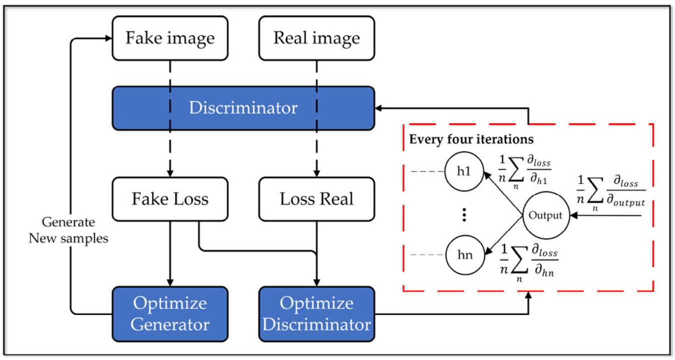

Figure 5. The asynchronous optimization scheme for the proposed model.

2.2.2. The Structure of T-CNN

In this paper, we have built a novel T-CNN model architecture for the PTCs curve classification and recognition task. The model construction process is based on a series of established design principles [35], and the settings of key parameters in the model have been adjusted according to the experimental results, including the number of convolutional layers, the size of the convolutional kernels, the stride, and the dropout parameters, among other factors. Eventually, the CNN model configuration with the best classification performance was selected as the final PTCs curve classification model.

The model's specific structure is as follows: the input layer inputs the augmented dataset generated by AoT-DCGAN. The feature extraction layer consists of three sets of stacked convolutional layers, with max-pooling applied after each convolutional layer. A dropout layer is added after the final convolutional layer to reduce overfitting in the neural network. The output layer comprises a fully-connected layer and a softmax layer, generating a probability distribution over possible classes. Specifically, the convolutional layers perform convolutions with a set of learnable filters or kernels to extract features and details from the PTCs curves. The max-pooling layers downsample the feature maps to reduce their size and increase training speed. Several techniques are applied to prevent overfitting, including the use of batch normalization layers for normalizing the feature maps and dropout layers that randomly discard a portion of the neuron outputs. The detailed structure of the T-CNN is illustrated in Figure 6.

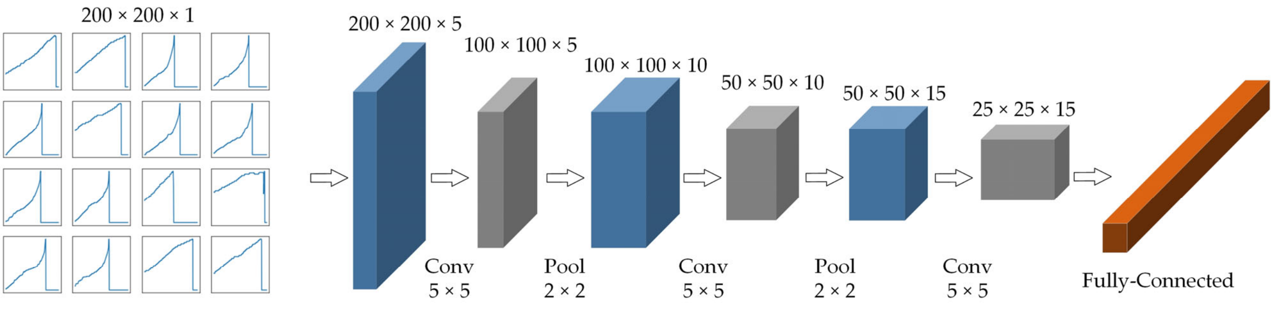

Figure 6. The detailed structure of the T-CNN.

3. Results

This section illustrates a series of comparative experiments to validate the superior performance of the proposed hybrid deep learning model, a combination of AoT-DCGAN and T-CNN, for PTCs curve classification. The efficacy of the proposed AoT-DCGAN weight optimization strategy was also confirmed. Various metrics such as recall and F1-score were used for evaluation, in addition to visualization techniques, like T-distributed stochastic neighbor embedding (T-SNE) and the confusion matrix, to provide a comprehensive view of the model's classification performance. Figure 7 presents the experimental flowchart. The detailed experimental procedure is as follows:

(1) Data acquisition: Original PTCs curves were generated via premium threaded connection make-up experiments.
(2) Dataset construction: The original dataset was expanded using AoT-DCGAN to generate four sets of datasets of varying quantities, based on the experimental requirements.
(3) Performance analysis: The performance of the proposed deep learning model was compared under different data augmentation ratios and classification models. Additionally, the reliability of the weight optimization strategy proposed in this study was validated.

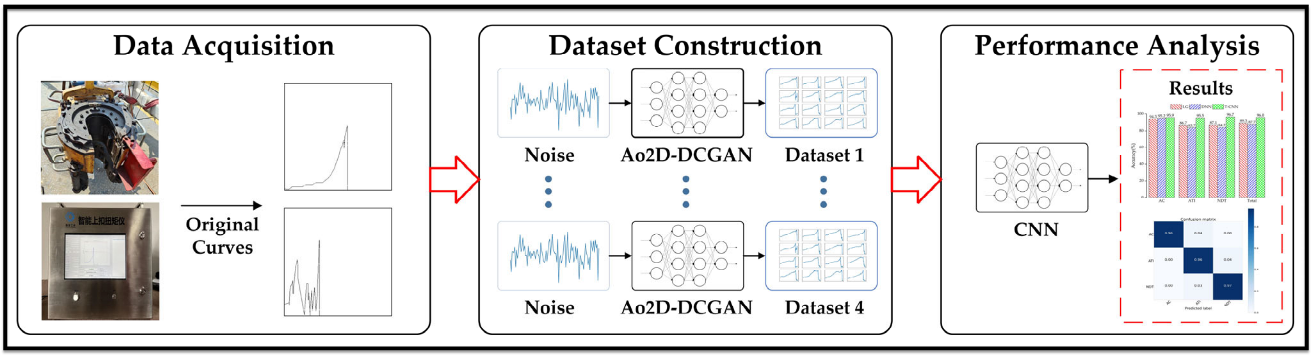

Figure 7. The flowchart of experiments.

3.1. Data Acquisition

The PTCs curve dataset used in this experiment was acquired from a series of premium threaded connection make-up experiments. Figure 8 illustrates the experimental procedure, which involves the initial make-up of PTCs on the tubing using hydraulic tongs, followed by the recording of the PTCs curves generated under varying make-up conditions using a torque recorder. The specific experimental equipment is depicted in Figure 9. The torque recorder collects the torque values and corresponding rotations generated during the make-up process at a frequency of 50 positions per turn. The hydraulic tube tong, used for making up the tubes, possessed a maximum make-up torque set at 3500 N.M and a make-up speed of 30 rpm. Three types of field make-up conditions were simulated: standard make-up, threaded damage make-up, and misalignment make-up. The specific dataset information is presented in Table 1, with a subset of samples shown in Figure 10.

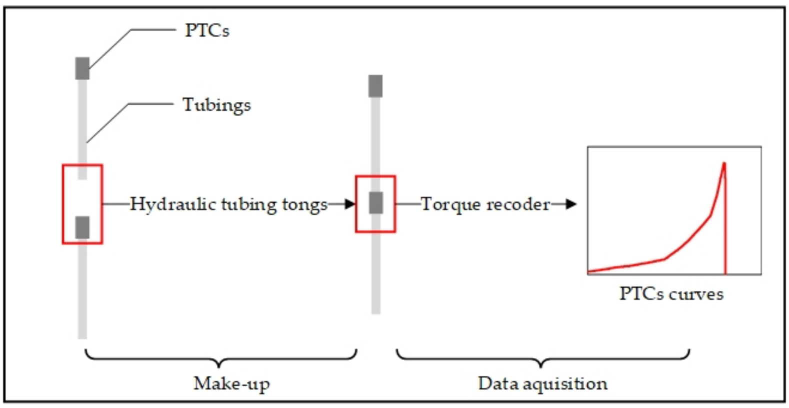

Figure 8. The make-up and data acquisition process.

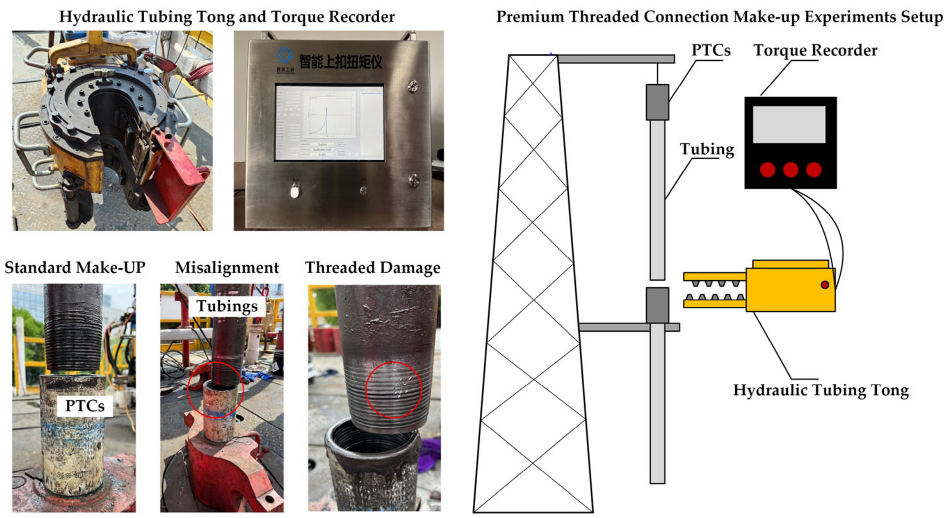

Figure 9. Experimental equipment and flowchart.

Table 1. Detailed dataset information.

Make-Up Conditions	Curve Description
Standard	Acceptable (AC)
Thread Damage	Abnormal Thread Interference (ATI)
Misalignment	None Defined Torque (NDT)

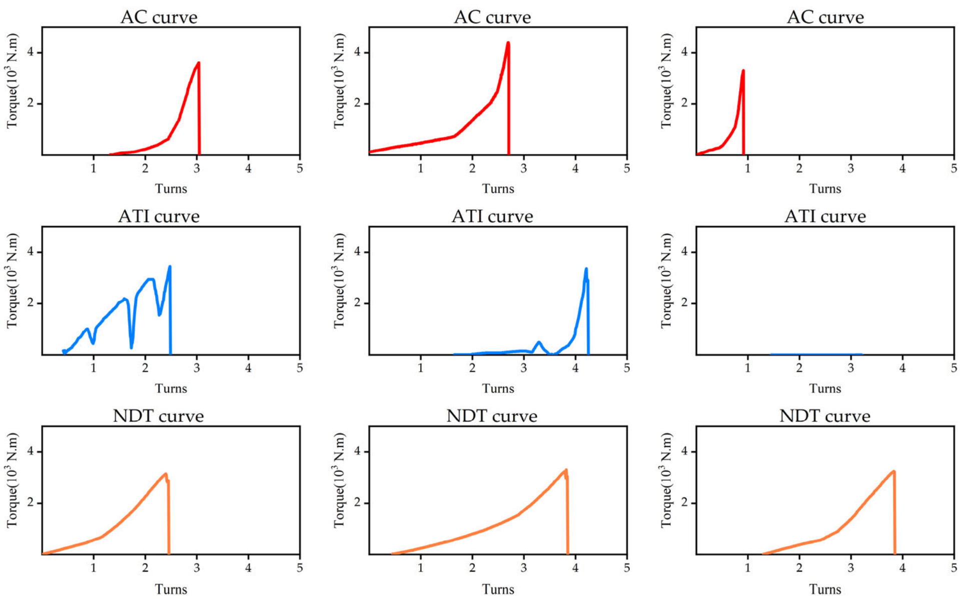

Figure 10. Examples of the PTCs curves from the experiments.

3.2. Dataset Construction

From the previously described experiments, a total of 600 original PTCs curves were produced, with each category consisting of 200 curves. This dataset, referred to as the original dataset, was utilized for generating synthetic PTCs curves via the AoT-DCGAN model and for subsequent comparative experiments in the classification model. A novel weight optimization strategy was employed to ensure the model's production of high-quality PTCs curves, facilitating asynchronous updates of the discriminator and generator weights. This strategy aimed to prevent the discriminator's loss function from becoming too small during early training stages, which could hinder weight updates. The AoT-DCGAN model generated a total of 600 synthetic PTCs curves using the original dataset, with each category containing 200 curves. The newly generated data was added to the original dataset, resulting in datasets with varying data augmentation ratios of 1.5, 1.75, and 2. In other words, the augmented datasets were 1.5 times, 1.75 times, and 2 times the size of the original dataset.

Figure 11 displays the artificial PTCs curves produced by the AoT-DCGAN under different operational conditions, with corresponding real data also presented. It can be observed that the curves generated by the model exhibit features similar to those of the real data. For instance, as shown in the ATI curves, the fluctuation characteristics of the real sample are accurately represented in the generated sample. Therefore, by this operation, it is possible to expand dataset with similar characteristics.

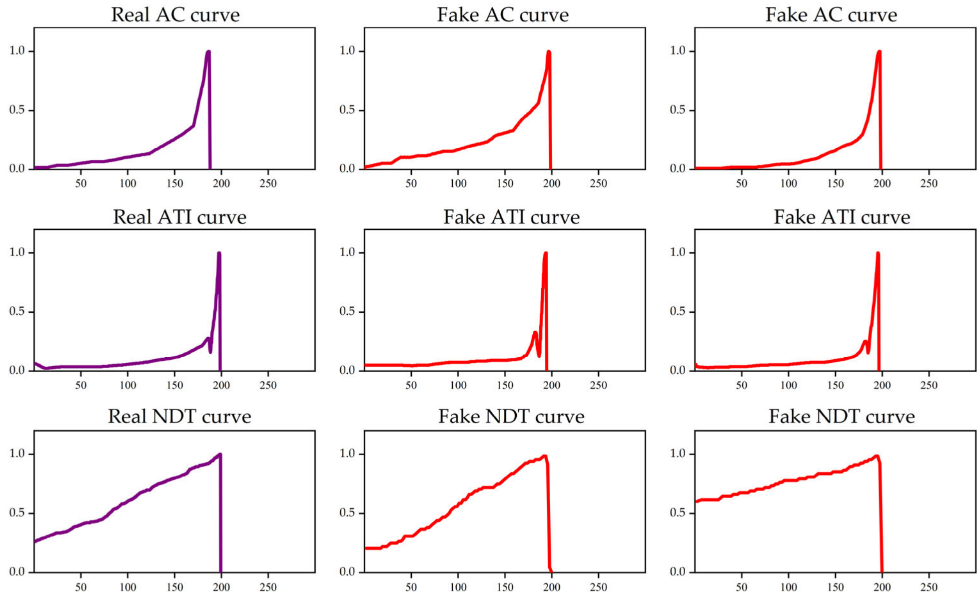

Figure 11. Examples of the real and fake data samples generated by AoT-DCGAN.

3.3. Performance Analysis

The experiments to validate the proposed hybrid model's superior performance in PTCs curve classification were conducted from three perspectives. Firstly, comparative experiments were performed with four groups of datasets of varying sizes to verify the classification performance of the proposed model under different data augmentation ratios. Secondly, comparative experiments were conducted with a set of classification models to demonstrate the superior performance of the T-CNN model proposed in this paper for PTCs curve classification under identical dataset conditions. Lastly, comparative experiments were performed with three groups of loss functions to examine the impact of the proposed asynchronous optimization strategy on enhancing the AoT-DCGAN's training process. The hyperparameters used in these experiments are listed in Table 2.

Table 2. Hyper-parameters used in the classification models.

Parameter	Description
Epochs	250
Batch size	16
Learning rate	0.002
Optimizer type	Adam
Shuffle	Every-epoch

In the four groups of comparative experiments on dataset sizes, the performance of the proposed hybrid model is demonstrated for data augmentation ratios of 600, 900, 1050, and 1200. Among these, the original dataset corresponds to 600, indicating the absence of data augmentation techniques, i.e., the AoT-DCGAN model. The datasets 900, 1050, and 1200 correspond to augmentation ratios of 1.5, 1.75, and 2, respectively. In each group, the training set accounts for 80% of the dataset, while the remaining 20% serves as the validation set. The classification performance of the models is evaluated using recall (Equation (4)), specificity (Equation (5)), F1-score (Equation (6)), and precision (Equation (7)). To mitigate the influence of randomness, the experimental results are averaged over five trials. The evaluation results of the models on different datasets can be seen in Tables 3–5.

$$\text{Recall} = \frac{\text{TP}}{\text{TP} + \text{FN}} \tag{4}$$

$$\text{Specificity} = \frac{\text{TN}}{\text{TN} + \text{FP}} \tag{5}$$

$$\text{F}_1\text{score} = 2 \times \frac{\text{precision} \times \text{recall}}{\text{precision} + \text{recall}} \tag{6}$$

$$\text{Precision} = \frac{\text{TP}}{\text{TP} + \text{FP}} \tag{7}$$

Table 3. Classification evaluation metrics for acceptable (AC) curves in different augmentation ratios.

Dataset Size	Recall	Specificity	F1-Score	Precision
600 (original)	92.4	85.9	85.5	79.5
900	93.6	94.3	92.1	90.7
1050	95.9	98.4	95.9	95.9
1200	**95.9**	**99.8**	**97.9**	**99.9**

Table 4. Classification evaluation metrics for abnormal interference (ATI) curves in different augmentation ratios.

Dataset Size	Recall	Specificity	F1-Score	Precision
600 (original)	76.3	95.7	81.7	87.9
900	85.5	95.3	86.8	88.1
1050	92.5	93.8	91.1	89.8
1200	**95.5**	**96.4**	**94.8**	**94.1**

Table 5. Classification evaluation metrics for none-defined torque (NDT) curves in different augmentation ratios.

Dataset Size	Recall	Specificity	F1-Score	Precision
600 (original)	73.0	89.4	75.5	78.1
900	84.1	92.3	84.5	85.0
1050	90.6	96.5	92.0	93.5
1200	**96.8**	**97.4**	**96.1**	**95.4**

As shown in Tables 3–5, for the AC curve, the classification performance with a dataset size of 1200 exhibits the best performance across all metrics, with 96%, 99.6%, 98%, and 99.3%, respectively. Similarly, for the ATI curve, the performance metrics outperform those of other groups when the dataset size is 1200, with 90.7%, 96.2%, 92.2%, and 93.7%, respectively. As for the NDT curve, the evaluation results indicate consistency with the previous results, all achieving the best performance when the dataset size is 1200, with percentages of 96.9%, 94.9%, 93.9%, and 91.2%.

To further demonstrate the ability of the AoT-DCGAN model to enhance the classification performance of PTCs curves, we utilized the T-SNE visualization method to depict the inherent structure and features of PTCs curves acquired by the T-CNN model at various data augmentation ratios in the softmax layer. As shown in Figure 12, the different colors of the data points represent samples in the dataset, where similar samples are closer to each other in the plot, and dissimilar samples are relatively farther apart. In Figure 12a, for the original dataset, the artificial features were not able to effectively cluster different types of curves, resulting in overlapping between different curves and indistinct data boundaries. However, as the data augmentation strength increased, as shown in Figure 12b–d, the artificial features gradually clustered different types of curves together, reducing the occurrence of overlapping between different curves, and presenting more distinct data boundaries.

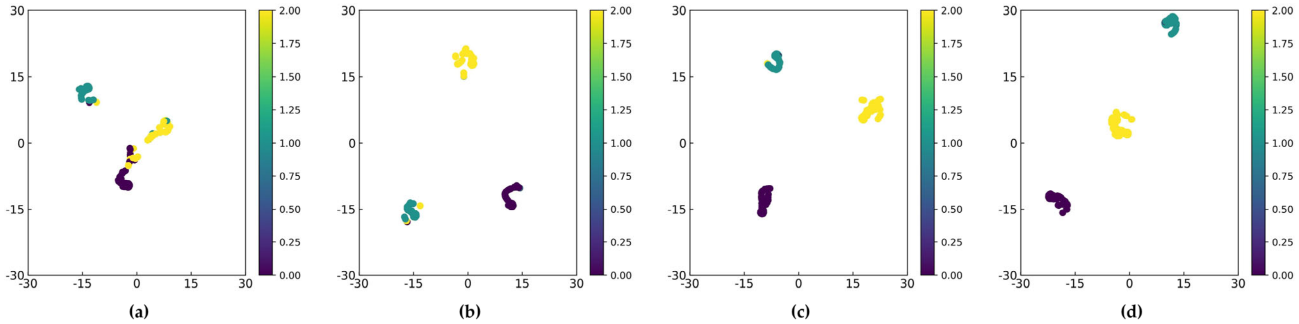

Figure 12. Feature visualization for different data augmentation ratios: (**a**) 600 dataset size; (**b**) 900 dataset size; (**c**) 1050 dataset size; (**d**) 1200 dataset size.

Figure 13 shows the confusion matrices results of the proposed model under different data augmentation intensities. The columns in the figure correspond to the predicted labels, while the rows correspond to the true labels. Each cell represents the combination of true and predicted classes, where the color indicates the accuracy of the predictions, with darker colors indicating greater accuracy. The results reveal that when the dataset size is 600, the model achieves the lowest prediction accuracy, with accuracies of 92%, 76%, and 73% for the classes AC, ATI, and NDT, respectively. Specifically, the model exhibits the highest misclassification rate between ATI and NDT, with 22% of ATI curves incorrectly identified as NDT. This could be attributed to the model's inability to differentiate the oscillatory characteristics of the ATI curves from the smooth features of the NDT curves due to insufficient training data. Additionally, 25% of the NDT curves are erroneously classified as AC curves, which might be caused by the indistinctive smooth features of some NDT curves, resembling those of AC curves. In cases of limited data, the model struggles to accurately extract their distinguishing features. As the dataset size increases, the model's performance in recognizing ATI and NDT improves. When the dataset size reaches 1200, the model achieves the best prediction accuracy for classes AC, ATI, and NDT, with accuracies of 96%, 96%, and 97%, respectively.

In one comparative experiment group, the performance of different classification models is compared when the dataset size is 1200. The models include a traditional machine learning model (logistic regression), a traditional deep learning model (deep neural network), and the T-CNN model designed in this paper. As shown in Figure 14, the results indicate that the proposed T-CNN outperforms the other models across all classes and in terms of overall accuracy, recording predictive accuracies of 95.9%, 95.5%, and 96.7%, with an overall accuracy of 96%. In contrast, although the DNN performs comparably to the other models in the AC curves, with a predictive accuracy of 95.2%, it reflects notably lower accuracies in the ATI and NDT curves, with values of 83.7% and 84.2%, respectively, leading to the lowest overall accuracy among the models at 87.7%. The performance of the LG model falls between that of the T-CNN and the DNN, with accuracies of 94.3%, 86.7%, and 87.1% in the AC, ATI, and NDT curves, respectively, and an overall accuracy of 89.3%.

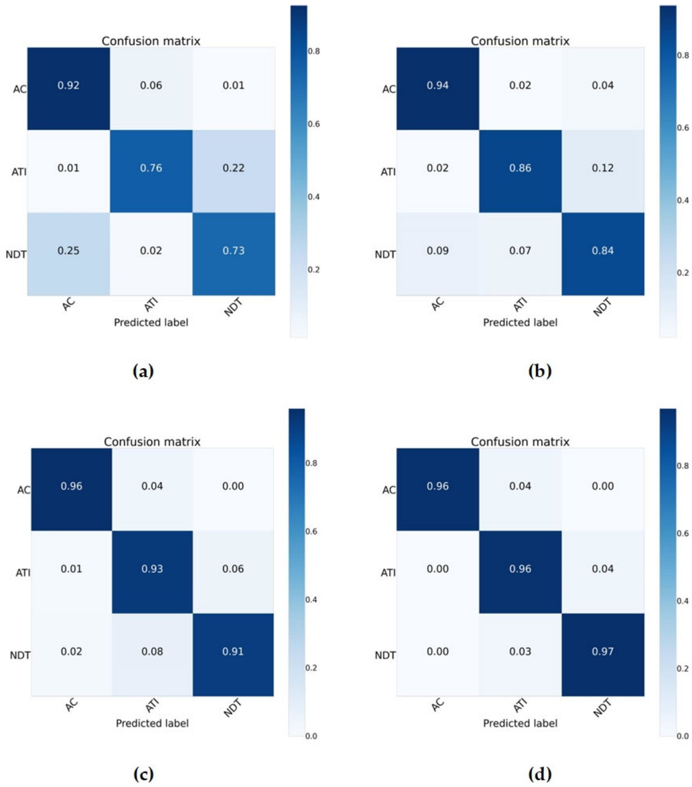

Figure 13. Confusion matrices for different data augmentation ratios: (**a**) 600 dataset size; (**b**) 900 dataset size; (**c**) 1050 dataset size; (**d**) 1200 dataset size.

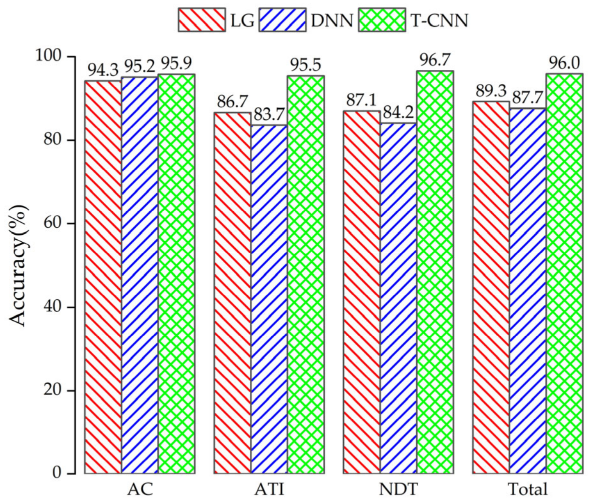

Figure 14. The comparison of recognition accuracy for each curve among the various network models.

In the three groups of comparative experiments on loss functions, the impact of the proposed weight optimization strategy on the model's loss functions for generating different types of PTCs curves is validated, as shown in Figures 15–17. It can be observed that for the AC, ATI, and NDT curves, when the weight optimization strategy is not used, the generator's loss function fails to decrease steadily. On the contrary, when the weight optimization strategy is employed, the generator's loss function decreases consistently, with increasing iterations, and eventually reaches a stable state. Additionally, the weight optimization strategy also has an effect on the discriminator's loss function, showing a smoother descent process.

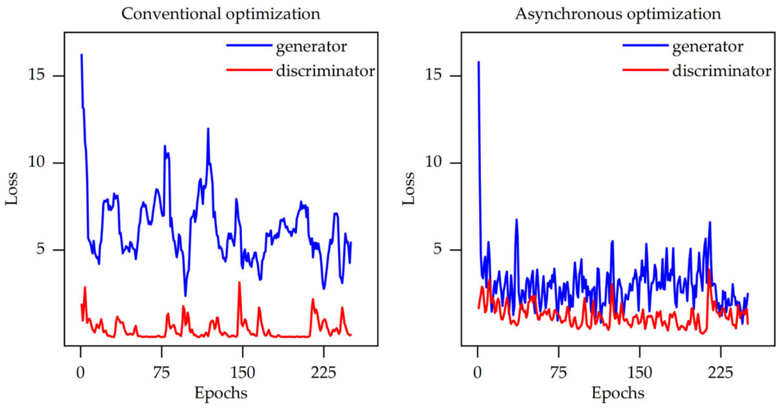

Figure 15. The loss functions of the DCGAN model for generating AC curves.

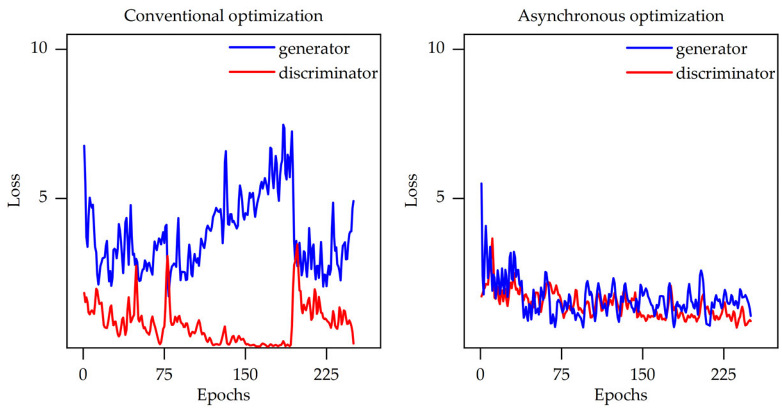

Figure 16. The loss functions of the DCGAN model for generating ATI curves.

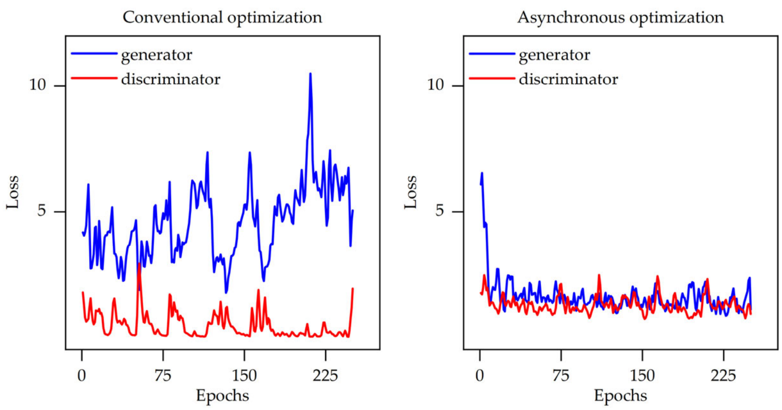

Figure 17. The loss functions of the DCGAN model for generating NDT curves.

4. Discussion

In this paper, we propose an improved AoT-DCGAN and T-CNN hybrid deep learning model for the automatic recognition and classification of PTCs curves, enabling the intelligent assessment of PTCs connection quality. The model addresses the following challenges: (1). achieving the automatic classification of PTCs curves; (2). overcoming the limited classification performance of deep learning models when dealing with small sample space; and (3). introducing a novel weight optimization strategy to mitigate the problem of gradient vanishing during the training process of the DCGAN model. To enable the automatic recognition of PTCs, we develop a novel T-CNN model that accurately classifies PTCs curves into different categories. To tackle the issue of small sample size, we design an AoT-DCGAN model to generate synthetic PTCs curves, thereby expanding the original dataset. Additionally, we employ the asynchronous optimization strategy to stabilize the gradient descent process of the generator, resulting in the generation of realistic synthetic PTCs curves.

Through a series of comparative experiments using different data augmentation ratios and traditional classification models, we found that the performance of the proposed method significantly improves as the dataset size increases, and the T-CNN demonstrates better performance for curve classification tasks. This conclusion is further supported by the T-SNE and confusion matrix visualization, which demonstrates a positive correlation between the model's clustering capability and the dataset size. Furthermore, we compared the variations in the loss function of the DCGAN model under different optimization strategies, and the results indicate that the proposed asynchronous optimization strategy greatly enhances the performance of the generator. In summary, the hybrid deep learning model proposed in this paper exhibits superior performance and significant potential in the evaluation of the connection quality in PTCs.

In addition, during the data generation process, it was observed that the weight update frequency and learning rate of the generator and discriminator in DCGAN have a significant impact on the results. Among these, the choice of learning rate has a more pronounced effect on the results. When a higher learning rate is used, the loss function decreases rapidly, but this can lead to the model being underfitted, preventing further optimization. Therefore, in future research, the application of dynamic learning rates in GAN models will be considered to address this issue.

Author Contributions: Conceptualization, Z.M.; methodology, Z.M. and J.S.; software, Z.M.; validation, J.S. and W.L.; formal analysis, Y.F.; investigation, Y.C.; resources, Y.F.; data curation, Z.M.; writing—original draft preparation, Z.M.; writing—review and editing, Z.M. and X.H.; visualization, Y.F.; supervision, Y.C.; project administration, Y.C.; funding acquisition, Y.F. All authors have read and agreed to the published version of the manuscript.

Funding: This research was funded by the Science and Technology Project of Oil & Gas and New Energy Company, PetroChina, grant number 20220302-09.

Institutional Review Board Statement: Not applicable.

Informed Consent Statement: Not applicable.

Data Availability Statement: Not applicable.

Conflicts of Interest: The authors declare no conflict of interest.

References

1. Guo, J.; Ma, F. Air tightness performance assessment of screw threads of oil tubings in high-sulfur gas wells in the Longgang Gas Field, Sichuan Basin. *Nat. Gas Ind.* **2013**, *33*, 128–131.
2. Huang, Y.; Zhang, Z.; Li, Y. Safety assessment of production casingin HTHP CO_2 gas well. *Drill. Prod. Technol.* **2014**, *37*, 78–81.
3. Jie, L.; Ye, H.; Hong, L. Technology and practice of well completion and putting into production for gas wells with high sulfur content in Sichuan and Chongqing areas. *Nat. Gas Ind.* **2006**, *26*, 72.
4. Chen, W.; Di, Q.; Zhang, H.; Chen, F.; Wang, W. The sealing mechanism of tubing and casing premium threaded connections under complex loads. *J. Pet. Sci. Eng.* **2018**, *171*, 724–730. [CrossRef]
5. Cui, F.; Li, W.; Wang, G.; Gu, Z.; Wang, Z. Design and study of gas-tight premium threads for tubing and casing. *J. Pet. Sci. Eng.* **2015**, *133*, 208–217.
6. Hao, L. The Structural Design of the Threaded Part of the Premium Connection Tubing. In Proceedings of the IOP Conference Series: Earth and Environmental Science, Kamakura, Japan, 10–11 October 2021; p. 052076.
7. Honglin, X.; Taihe, S.; Zhi, Z. Theoretical analysis on makeup torque in tubing and casing premium threaded connections. *J. Southwest Pet. Univ. (Sci. Technol. Ed.)* **2014**, *36*, 160.
8. Yang, B.; Xu, H.; Xiang, S.; Zhang, Z.; Su, K.; Yang, Y. Effects of Make-Up Torque on the Sealability of Sphere-Type Premium Connection for Tubing and Casing Strings. *Processes* **2023**, *11*, 256. [CrossRef]
9. Ma, Z.-H.; Fan, Y.; Zhang, H.-L.; Tang, G.; Li, Y.-F.; Wang, C.-L.; Peng, G.; Duan, Y.-Q. Research on Evaluation Method of Make-Up Torque of Premium Thread Based on Logistic Regression. In *Proceedings of the International Field Exploration and Development Conference*; Springer: Singapore, 2021; pp. 3840–3853.

10. Rawat, W.; Wang, Z.H. Deep Convolutional Neural Networks for Image Classification: A Comprehensive Review. *Neural Comput.* **2017**, *29*, 2352–2449. [CrossRef]
11. Qin, J.; Pan, W.; Xiang, X.; Tan, Y.; Hou, G. A biological image classification method based on improved CNN. *Ecol. Inform.* **2020**, *58*, 101093. [CrossRef]
12. Yuan, Y.; Mou, L.; Lu, X. Scene recognition by manifold regularized deep learning architecture. *IEEE Trans. Neural Netw. Learn. Syst.* **2015**, *26*, 2222–2233.
13. Acharya, U.R.; Fujita, H.; Oh, S.L.; Hagiwara, Y.; Tan, J.H.; Adam, M. Application of deep convolutional neural network for automated detection of myocardial infarction using ECG signals. *Inf. Sci.* **2017**, *415*, 190–198. [CrossRef]
14. Athamanolap, P.; Parekh, V.; Fraley, S.I.; Agarwal, V.; Shin, D.J.; Jacobs, M.A.; Wang, T.H.; Yang, S. Trainable High Resolution Melt Curve Machine Learning Classifier for Large-Scale Reliable Genotyping of Sequence Variants. *PLoS ONE* **2014**, *9*, e109094. [CrossRef]
15. Jiao, J.Y.; Zhao, M.; Lin, J.; Liang, K.X. A comprehensive review on convolutional neural network in machine fault diagnosis. *Neurocomputing* **2020**, *417*, 36–63. [CrossRef]
16. Ozkok, F.O.; Celik, M. Convolutional neural network analysis of recurrence plots for high resolution melting classification. *Comput. Methods Programs Biomed.* **2021**, *207*, 106139. [CrossRef]
17. Jing, L.Y.; Zhao, M.; Li, P.; Xu, X.Q. A convolutional neural network based feature learning and fault diagnosis method for the condition monitoring of gearbox. *Measurement* **2017**, *111*, 1–10. [CrossRef]
18. Peng, Y. Artificial intelligence applied in sucker rod pumping wells: Intelligent dynamometer card generation, diagnosis, and failure detection using deep neural networks. In Proceedings of the SPE Annual Technical Conference and Exhibition, Calgary, AB, Canada, 30 September–2 October 2019.
19. Zhang, R.; Wang, L.; Chen, D. An Intelligent Diagnosis Method of the Working Conditions in Sucker-Rod Pump Wells Based on Convolutional Neural Networks and Transfer Learning. *Energy Eng.* **2021**, *118*, 1069–1082. [CrossRef]
20. Tang, S.N.; Yuan, S.Q.; Zhu, Y. Convolutional Neural Network in Intelligent Fault Diagnosis Toward Rotatory Machinery. *IEEE Access* **2020**, *8*, 86510–86519. [CrossRef]
21. Shorten, C.; Khoshgoftaar, T.M. A survey on image data augmentation for deep learning. *J. Big Data* **2019**, *6*, 60. [CrossRef]
22. Sun, C.; Shrivastava, A.; Singh, S.; Gupta, A. Revisiting unreasonable effectiveness of data in deep learning era. In Proceedings of the IEEE International Conference on Computer Vision, Venice, Italy, 22–29 October 2017; pp. 843–852.
23. Goodfellow, I.; Pouget-Abadie, J.; Mirza, M.; Xu, B.; Warde-Farley, D.; Ozair, S.; Courville, A.; Bengio, Y. Generative adversarial nets. *Adv. Neural Inf. Process. Syst.* **2014**, *27*, 139–144.
24. Liang, P.; Deng, C.; Wu, J.; Li, G.; Yang, Z.; Wang, Y. Intelligent fault diagnosis via semisupervised generative adversarial nets and wavelet transform. *IEEE Trans. Instrum. Meas.* **2019**, *69*, 4659–4671. [CrossRef]
25. Wu, Q.; Chen, Y.; Meng, J. DCGAN-based data augmentation for tomato leaf disease identification. *IEEE Access* **2020**, *8*, 98716–98728. [CrossRef]
26. Zhang, T.C.; Chen, J.L.; Li, F.D.; Pan, T.Y.; He, S.L. A Small Sample Focused Intelligent Fault Diagnosis Scheme of Machines via Multimodules Learning With Gradient Penalized Generative Adversarial Networks. *IEEE Trans. Ind. Electron.* **2021**, *68*, 10130–10141. [CrossRef]
27. Zhang, W.; Li, X.; Jia, X.D.; Ma, H.; Luo, Z.; Li, X. Machinery fault diagnosis with imbalanced data using deep generative adversarial networks. *Measurement* **2020**, *152*, 107377. [CrossRef]
28. Zhang, Y.Q.; Han, J.L.; Jing, L.Y.; Wang, C.M.; Zhao, L. Intelligent Fault Diagnosis of Broken Wires for Steel Wire Ropes Based on Generative Adversarial Nets. *Appl. Sci.* **2022**, *12*, 11552. [CrossRef]
29. Gui, J.; Sun, Z.A.; Wen, Y.G.; Tao, D.C.; Ye, J.P. A Review on Generative Adversarial Networks: Algorithms, Theory, and Applications. *IEEE Trans. Knowl. Data Eng.* **2023**, *35*, 3313–3332. [CrossRef]
30. Wang, R.; Zhang, S.; Chen, Z.; Li, W. Enhanced generative adversarial network for extremely imbalanced fault diagnosis of rotating machine. *Measurement* **2021**, *180*, 109467. [CrossRef]
31. Li, Z.; Zheng, T.; Wang, Y.; Cao, Z.; Guo, Z.; Fu, H. A novel method for imbalanced fault diagnosis of rotating machinery based on generative adversarial networks. *IEEE Trans. Instrum. Meas.* **2020**, *70*, 1–17. [CrossRef]
32. Yu, Y.; Cao, Y.; Qu, Z.; Dou, Y.; Wang, Z. Finite-Element Analysis on Energy Dissipation and Sealability of Premium Connections under Dynamic Loads. *Processes* **2023**, *11*, 1927. [CrossRef]
33. Yu, H.; Wang, H.; Lian, Z. An Assessment of Seal Ability of Tubing Threaded Connections: A Hybrid Empirical-Numerical Method. *J. Energy Resour. Technol.* **2023**, *145*, 052902. [CrossRef]
34. Creswell, A.; White, T.; Dumoulin, V.; Arulkumaran, K.; Sengupta, B.; Bharath, A.A. Generative Adversarial Networks An overview. *Ieee Signal Process. Mag.* **2018**, *35*, 53–65. [CrossRef]
35. Abdel-Hamid, O.; Deng, L.; Yu, D. Exploring convolutional neural network structures and optimization techniques for speech recognition. In Proceedings of the Interspeech, Lyon, France, 25–29 August 2013; pp. 1173–1175.

Disclaimer/Publisher's Note: The statements, opinions and data contained in all publications are solely those of the individual author(s) and contributor(s) and not of MDPI and/or the editor(s). MDPI and/or the editor(s) disclaim responsibility for any injury to people or property resulting from any ideas, methods, instructions or products referred to in the content.